SUSD4 Controls Activity-Dependent Degradation of AMPA Receptor GLUA2 and Synaptic Plasticity

I. González-Calvo[1,2,†], K. Iyer[1,†], M. Carquin[1], A. Khayachi[1], F.A. Giuliani[2], J. Vincent[3], M. Séveno[4], S.M. Sigoillot[1], M. Veleanu[1], S. Tahraoui[1], M. Albert[1], O. Vigy[5], Y. Nadjar[6], A. Dumoulin[6], A. Triller[6], J.-L. Bessereau[7], L. Rondi-Reig[3], P. Isope[2], F. Selimi[1]*

Affiliations:

[1] Center for Interdisciplinary Research in Biology (CIRB), Collège de France, CNRS, INSERM, PSL Research University, Paris, France.

[2] Institut de Neurosciences Cellulaires et Intégratives (INCI), CNRS, Université de Strasbourg, , Strasbourg, France.

[3] Institut Biology Paris Seine (IBPS), Neuroscience Paris Seine (NPS), CeZaMe, CNRS, Sorbonne University, INSERM, Paris, France.

[4] BioCampus Montpellier, CNRS, INSERM, Université de Montpellier, Montpellier, France.

[5] Institut de Génomique Fonctionnelle, CNRS, INSERM, Université de Montpellier, Montpellier, France.

[6] École Normale Supérieure, Institut de Biologie de l'ENS, INSERM, CNRS, PSL Research University, Paris, France.

[7] Université de Lyon, Université Claude Bernard Lyon 1, CNRS UMR 5310, INSERM U 1217, Institut Neuromyogène, 69008, Lyon, France.

* Correspondence to: fekrije.selimi@college-de-france.fr

† Equal contribution.

Summary

At excitatory synapses, the choice between recycling or degradation of glutamate AMPA receptors controls the direction of synaptic plasticity. In this context, how the degradation machinery is targeted to specific synaptic substrates in an activity-dependent manner is not understood. Here we show that SUSD4, a complement-related transmembrane protein, is a tether for HECT ubiquitin ligases of the NEDD4 subfamily, which promote the degradation of a large number of cellular substrates. SUSD4 is expressed by many neuronal populations starting at the time of synapse formation. Loss-of-function of *Susd4* in the mouse prevents activity-dependent degradation of the GLUA2 AMPA receptor subunit and long-term depression at cerebellar synapses, and leads to impairment in motor coordination adaptation and learning. SUSD4 could thus act as an adaptor targeting NEDD4 ubiquitin ligases to AMPA receptors during long-term synaptic plasticity. These findings shed light on the potential contribution of *SUSD4* mutations to the etiology of neurodevelopmental diseases.

Introduction

AMPA-type glutamate receptors are responsible for fast excitatory transmission in the central nervous system. Fine-tuning of their properties and their synaptic numbers underlies synapse maturation and synapse plasticity and is central to proper circuit function and behavior (Anggono and Huganir, 2012; Diering and Huganir, 2018; Kessels and Malinow, 2009). Long-term synaptic plasticity has been proposed to underlie learning and memory (Collingridge et al., 2010; Nicoll, 2017). Synaptic strength can be either decreased (long-term depression, LTD) or increased (long-term potentiation, LTP) depending on the timing and pattern of neuronal activity in a network. Defects in the regulation of long-term synaptic plasticity and AMPA receptors could contribute to a range of brain diseases such as epilepsy, intellectual deficiencies and autism spectrum disorders (ASDs). Long-term synaptic plasticity deficits are a common phenotype of many mice models for intellectual disabilities and ASDs (Baudouin et al., 2012; Piochon et al., 2014; Volk et al., 2015). Mutations in genes coding for AMPA receptor subunits (Davies et al., 2017; Martin et al., 2017; Salpietro et al., 2019; Satterstrom et al., 2018) or their regulatory subunits (Brechet et al., 2017; Chiu et al., 2017) have been found in patients with neurodevelopmental disorders.

The modification of AMPA receptor numbers at synapses is a highly dynamic process, involving regulation of receptor diffusion (Choquet and Triller, 2013; Penn et al., 2017), their insertion in the plasma membrane, anchoring at the postsynaptic density and endocytosis (Anggono and Huganir, 2012). After activity-dependent endocytosis, AMPA receptors are either recycled to the plasma membrane or targeted to the endolysosomal compartment for degradation (Ehlers, 2000; Lee et al., 2004; Park et al., 2004). The decision between these two fates regulates the direction of synaptic plasticity. Recycling promotes LTP and relies on many molecules, such as GRASP1, GRIP1, PICK1 and NSF (Anggono and Huganir, 2012). Targeting to the endolysosomal compartment and degradation promote LTD (Fernandez-Monreal et al., 2012; Kim et al., 2017; Matsuda et al., 2013), but the regulation of the targeting and degradation process remains poorly understood. One mechanism that regulates activity-dependent degradation of synaptic proteins is ubiquitination, a major post-translational modification (Cajigas et al., 2010). Both GLUA1 and GLUA2 AMPA receptor subunits have been shown to be ubiquitinated in an activity-dependent manner (Lussier et al., 2011; Schwarz et al., 2010; Widagdo et al., 2015). A major remaining question however is how AMPA receptor degradation is specifically controlled given the large number of substrates for E3 ubiquitin ligases in cells, and the spatio-temporal specificity required for proper synaptic plasticity in neurons.

The *SUSD4* gene is located in a genomic region deleted in patients with the 1q41q42 syndrome that includes developmental delays and intellectual deficiency (Rosenfeld et al., 2011). *SUSD4* has been identified recently as one of the 124 genes enriched in *de novo* missense mutations in a large cohort of individuals with ASDs or intellectual deficiencies (Coe et al., 2019). A copy number variation and several *de novo* mutations with a high CADD score, which indicates the deleteriousness of the mutations, have been described in the *SUSD4* gene in patients with ASDs ((Cuscó et al., 2009); denovo-db, Seattle, WA (denovo-db.gs.washington.edu) 10, 2019). The mammalian *Susd4* gene codes for a transmembrane protein with four extracellular CCP (complement control protein) domains (**Figure 1A**) and is highly expressed in the central nervous system (Holmquist et al., 2013). The CCP domain, also known as Sushi domain, is evolutionarily conserved and found in several proteins with synaptic function. Acetylcholine receptor clustering is regulated by CCP-containing proteins in *Caenorhabditis elegans* (Gendrel et al., 2009) and in *Drosophila melanogaster* (Nakayama et al., 2016). In humans, mutations in the CCP domain-

containing secreted protein SRPX2 are associated with epilepsy and speech dysfunction, and SRPX2 knockdown leads to decreased synapse number and vocalization in mice (Sia et al., 2013). Despite the increase in the diversity of CCP domain-containing proteins in evolution (18 in *C. elegans* and 198 in humans; smart.embl.de), the function of many of the CCP domain-containing proteins remains unknown. The only described role for the SUSD4 protein is its ability to regulate complement system activation in erythrocytes by binding the C1Q domain (Holmquist et al., 2013). Interestingly, the C1Q globular domain is found in major synaptic regulators such as C1QA (Stevens et al., 2007), CBLNs (Matsuda et al., 2010; Uemura et al., 2010) and C1Q-like proteins (Bolliger et al., 2011; Kakegawa et al., 2015; Sigoillot et al., 2015). Altogether these studies point to a potential role of SUSD4 in synapse formation and/or function and in the etiology of several neurodevelopmental disorders.

Proper development and function of the cerebellar circuitry is central for motor coordination and adaptation, and a range of cognitive tasks (Badura et al., 2018; Hirai et al., 2005; Ichise et al., 2000; Lefort et al., 2019; Rochefort et al., 2011; Tsai et al., 2012), and cerebellar dysfunction is associated with several neurodevelopmental disorders including ASDs (Stoodley, 2016; Stoodley et al., 2018; Wang et al., 2014). Cerebellar Purkinje cells (PCs) receive more than a hundred thousand parallel fiber (PF) synapses whose formation, maintenance and plasticity are essential for cerebellar-dependent learning (Gutierrez-Castellanos et al., 2017; Hirai et al., 2005; Ito, 2006; Kashiwabuchi et al., 1995). Postsynaptic LTD was first described at synapses between PFs and cerebellar PCs (Gao et al., 2012; Hirano, 2018; Ito, 2001; Ito and Kano, 1982), where it can be induced by conjunctive stimulation of PFs with the other excitatory input received by PCs, the climbing fiber (CF) (Coesmans et al., 2004; Ito, 2001; Suvrathan et al., 2016). The function of members of the C1Q family, such as CBLN1 and C1QL1, is essential for excitatory synapse formation and LTD in cerebellar PCs (Hirai et al., 2005; Kakegawa et al., 2015; Matsuda et al., 2010; Sigoillot et al., 2015; Uemura et al., 2010), suggesting that proteins, such as SUSD4, that interact with the C1Q globular domain could regulate these processes. PF LTD is dependent on AMPA receptor endocytosis, in particular the GLUA2 subunit (Chung et al., 2003; Xia et al., 2000), and their targeting to RAB7 compartments (Kim et al., 2017). However, the mechanism regulating AMPA receptor targeting to the endolysosomal compartment at PF synapses, as at other synapses, remains unknown.

To identify the role of SUSD4 in brain development and function, we thus analyzed the phenotype of a *Susd4* loss-of-function mouse model in the cerebellum. We found that knockout of the *Susd4* gene leads to impaired synaptic LTD in cerebellar PCs and deficits in motor coordination and adaptation learning. Using affinity-purification followed by proteomics analysis and biochemical assays, we show that the SUSD4 protein binds E3 ubiquitin ligases of the NEDD4 family and regulates activity-dependent degradation of GLUA2 receptors. Because of the domain structure of SUSD4, our results suggest a new regulatory mechanism that can bring spatio-temporal specificity to the degradation machinery in neurons, allowing proper synaptic plasticity and learning.

Results

Susd4 is broadly expressed in neurons during postnatal development

Given the potential synaptic role for SUSD4, its pattern of expression should correlate with the timing of synapse formation and/or maturation during postnatal development. *In situ* hybridization experiments using mouse brain sections showed high expression of *Susd4* mRNA in neurons in

many regions of the central nervous system, including the cerebral cortex, the hippocampus, the cerebellum and the brainstem (**Figure 1** and **S1**). *Susd4* expression was already detected by postnatal day 0 (P0) in some regions, but increased with brain maturation (**Figure S1**). In the cerebellum, a structure where the developmental sequence leading to circuit formation and maturation is well described (Sotelo, 2004), quantitative RT-PCR showed that *Susd4* mRNA levels start increasing at P7 and by P21 reach about 15 times the levels detected at birth (**Figure 1B**). At P7, a major increase in synaptogenesis is observed in the cerebellum, due to the formation of hundreds of thousands of PF excitatory synapses on the distal dendritic spines of each PC, and the translocation of a single CF arising from an inferior olivary neuron that forms about 300 excitatory synapses on proximal PC dendrites (Leto et al., 2016). In the brainstem, where cell bodies of inferior olivary neurons are located, the increase in *Susd4* mRNA occurs earlier, already by P3, in parallel with the rate of synaptogenesis increasing during the first postnatal week in the inferior olive (Gotow and Sotelo, 1987). To identify the subcellular localization of the SUSD4 protein and because of the lack of suitable antibodies for immunolabeling, viral particles enabling CRE-dependent coexpression of HA-tagged SUSD4 and GFP in neurons were injected in the cerebellum of adult mice expressing the CRE recombinase specifically in cerebellar PCs. Immunofluorescent labeling against the HA tag demonstrated the presence of tagged SUSD4 in dendrites and distal dendritic spines that are the postsynaptic compartments of PF synapses in PCs (**Figure 1C**). Thus, its timing of expression during postnatal development and its subcellular localization in cerebellar PCs support a role for SUSD4 in excitatory synapse formation and/or function.

Susd4 loss-of-function leads to deficits in motor coordination and learning

To determine the synaptic function of SUSD4, we analyzed the phenotype of constitutive knockout (KO) mice completely lacking expression of *Susd4* mRNA due to deletion of exon 1 (**Figure 1D, 1E** and **S2**). No obvious alterations of mouse development and behavior were detected in those mutants, an observation that was confirmed by assessment of their physical characteristics (weight, piloerection, cf. **Table S1**), basic behavioral abilities such as sensorimotor reflexes (whisker responses, eye blinking, cf. **Table S1**) and motor responses (open field locomotion, cf. **Table S1**). Because of the high *Susd4* expression in the olivocerebellar system (**Figure 1** and **S1**), we further assessed the behavior of *Susd4* KO mice for two abilities well known to depend on normal function of this network, motor coordination and motor learning (Kayakabe et al., 2014; Lalonde and Strazielle, 2001; Rondi-Reig et al., 1997). Using a footprint test, a slightly larger print separation of the front and hind paws in the *Susd4* KO mice was detected but no differences in the stride length and stance width were found (**Figure S3**). In the accelerated rotarod assay, a classical test of motor adaptation and learning (Buitrago et al., 2004), the mice were tested three times per day at one hour interval during five consecutive days. The *Susd4* KO mice performed as well as the wild-type (WT) controls on the first trial, indicating that there is no deficit in their balance function (**Figure 1F**), despite the slight change in fine motor coordination found in the footprint test. However, while the WT mice improved their performance as early as the third trial on the first day, and further improved with several days of training, no learning could be observed for the *Susd4* KO mice either during the first day, or in the following days. These results show that *Susd4* loss-of-function leads to impaired motor coordination and learning in adult mice.

***Susd4* loss-of-function prevents long-term depression at cerebellar parallel fiber/Purkinje cell synapses**

Motor coordination and learning are deficient when cerebellar development is impaired (Hirai et al., 2005; Ichise et al., 2000; Tsai et al., 2012; Zuo et al., 1997). No deficits in the global cytoarchitecture of the cerebellum and morphology of PCs were found in *Susd4* KO mice (**Figure S4**). Using high density microelectrode array, we assessed the spontaneous activity of PCs in acute cerebellar slices from *Susd4* KO compared to WT (**Figure S5**). No differences were detected in either the mean spiking frequency, the coefficient of variation of interspike intervals (CV) and the intrinsic variability of spike trains (CV2, (Holt and Douglas, 1996) showing that the firing properties of PCs are not affected by *Susd4* loss-of-function.

Co-immunolabeling of parallel fiber presynaptic boutons using an anti-VGLUT1 antibody and PCs using an anti-calbindin antibody in cerebellar sections from juvenile WT mice revealed an extremely dense staining in the molecular layer corresponding to the highly numerous parallel fibers contacting PC distal dendritic spines (**Figure 2A**). The labeling pattern was similar in *Susd4* KO and high-resolution microscopy and quantitative analysis confirmed that there are no significant changes in the mean density and volume of VGLUT1 clusters following *Susd4* loss-of-function (**Figure 2A**). Electric stimulation of increasing intensity in the molecular layer allows the progressive recruitment of the PFs (Konnerth et al., 1990), and can be used to assess the number of synapses and the basic PF/PC transmission using whole-cell patch-clamp recordings of PCs on acute cerebellar slices (**Figure 2B**). No difference was observed in the amplitude and the kinetics of the responses to PF stimulation in PCs from *Susd4* KO and control mice (**Figure 2C** and **Figure S6**). Furthermore, the probability of vesicular release in the presynaptic PF bouton, as assessed by measurements of paired pulse facilitation (Atluri and Regehr, 1996; Konnerth et al., 1990; Valera et al., 2012), was not changed at PF/PC synapses (**Figure 2C**). Finally, no differences in the frequency and amplitude of evoked quantal events were detected (**Figure S6**). Thus, in accordance with the morphological analysis, there is no major effect of *Susd4* invalidation on the number and basal transmission of PF/PC synapses.

Long-term synaptic plasticity of PF/PC synapses is involved in proper motor coordination and adaptation learning (Gutierrez-Castellanos et al., 2017; Hirano, 2018; Kakegawa et al., 2018). We first assessed LTD in PF/PC synapses using conjunctive stimulation of PFs and CFs and whole-cell patch-clamp recordings of PCs in acute cerebellar slices from juvenile mice. Our protocol induced a 42% average decrease in the amplitude of PF excitatory postsynaptic currents (EPSCs) in PCs from WT mice while the paired pulse facilitation ratio was not changed during the course of our recordings (**Figure 2D** and **Figure S6**). In *Susd4* KO PCs, the same LTD induction protocol did not induce any significant change in PF EPSCs during the 30 minutes recording period, showing that LTD is greatly impaired in the absence of SUSD4 (**Figure 2D**). LTP can be induced by high frequency stimulation of parallel fibers only, and is also involved in cerebellar dependent-learning (Binda et al., 2016; Gutierrez-Castellanos et al., 2017). In control mice, tetanic stimulation during 5 minutes induced a transient increase in transmission of about 20% and the amplitude of the response returned to baseline after only 15 minutes (**Figure 2E** and **Figure S6**). However, in the case of *Susd4* KO PCs, the same protocol induced a 27% increase in transmission that was maintained after 35 minutes (**Figure 2E)**, indicating a facilitation of LTP of PF/PC synapses in the absence of *Susd4* expression.

Lack of LTD of PF/PC synapses could arise from deficient CF transmission. To test this possibility, we first crossed the *Susd4* knockout mice with the Htr5b-GFP BAC transgenic line

(www.gensat.org) expressing soluble GFP specifically in inferior olivary neurons in the olivocerebellar system to visualize CFs. We found that CFs had a normal morphology and translocated along the proximal dendrites of their PC target in *Susd4* KO mice (**Figure 3A**). We then assessed whether developmental elimination of supernumerary CFs was affected by *Susd4* invalidation using whole-cell patch-clamp recordings of PCs on cerebellar acute slices (Crepel et al., 1976; Hashimoto and Kano, 2003). No difference was found in the percentage of remaining multiply-innervated PCs in the absence of *Susd4* (**Figure 3B**). We next used VGLUT2 immunostaining to label CF presynaptic boutons and analyze their morphology using high resolution confocal microscopy and quantitative image analysis. VGLUT2 immunostaining revealed the typical CF innervation territory on PC proximal dendrites, extending up to about 80% of the molecular layer height both in control and *Susd4* KO mice (**Figure 3C**). Furthermore, the number and density of VGLUT2 clusters were not significantly different between WT and *Susd4* KO mice. To test whether the lack of PF LTD was due to deficient CF transmission, we used whole-cell patch-clamp recordings of PCs in acute cerebellar slices. Contrary to what could have been expected, the typical all-or-none climbing fiber evoked EPSC was detected in PCs from *Susd4* KO mice with similar kinetics (**Figure S7**), but with increased amplitude when compared to WT PCs (**Figure 3D**). Thus, the lack of CF-dependent PF/PC synapse LTD in *Susd4* KO mice is not due to reduced CF/PC synapse formation or transmission. Measurements of evoked quantal events revealed an increase in the amplitude of the quantal EPSCs at CF/PC synapses from juvenile mice (**Figure 3E** and **S7**). In *Susd4* KO, paired-pulse facilitation and depression at PF/PC and CF/PC synapses, respectively, are normal both in basal conditions and after plasticity induction (**Figures 2C, 3D, S6D** and **S6F**) suggesting that the changes in PF/PC synaptic plasticity and in CF/PC transmission in *Susd4* KO PCs have a postsynaptic origin. Overall our results show that *Susd4* loss-of-function in mice leads to a highly specific phenotype characterized by lack of postsynaptic LTD in the absence of defects in synaptogenesis and in basal transmission in PCs.

SUSD4 binds to HECT E3 ubiquitin ligases

What are the mechanisms that could allow control of long-term synaptic plasticity by SUSD4? We searched for SUSD4 molecular partners by affinity-purification of cerebellar synaptosome extracts using GFP-tagged SUSD4 as a bait (**Figure 4A**), followed by proteomic identification of interacting partners by liquid chromatography with tandem mass spectrometry (LC-MS/MS; Savas et al., 2014). Twenty-eight candidates were identified, several of which were functionally linked to ubiquitin ligase activity by gene ontology term analysis (**Figure 4A** and **Table 1**). Immunoblot analysis of affinity-purified extracts confirmed the interaction of SUSD4 with several members of the HECT E3 ubiquitin ligases of the NEDD4 subfamily (**Figure 4C**). Removal of the intracellular domain of SUSD4 (SUSD4-ΔC_T mutant) prevented this interaction proving the specificity of SUSD4 binding (**Figure 4B** and **C**). Ubiquitin ligases of the NEDD4 family bind variants of PY motifs on target substrates and adaptors (Chen et al., 2017). Two potential PY binding sites are present in the intracellular tail of SUSD4 (**Figure 4B**). To test whether these sites mediate interaction between SUSD4 and NEDD4 ubiquitin ligases, we generated single- and double- point mutants of SUSD4 and tested their ability to interact with NEDD4 ligases in transfected HEK293 cells. While the mutation of the PPxY site (SUSD4-ΔPY mutant) abrogated binding of SUSD4 only partially, mutation of only the LPxY site (SUSD4-ΔLY mutant) or of both sites (SUSD4-ΔPY/LY mutant) completely prevented the binding to NEDD4 ubiquitin ligases (**Figure 4D**). These mutations did not change the level of SUSD4 expression in transfected HEK293 cells

suggesting that SUSD4 itself is not a substrate for NEDD4 ubiquitin ligases. Interestingly, NEDD4 ubiquitin ligases are autoinhibited by binding of the HECT domain to their WW domains. Interaction of regulatory proteins with these WW domains has been shown to release autoinhibition and allow ubiquitination of substrates by the NEDD4 ubiquitin ligases (Wang et al., 2019). Thus, our results suggest that while the LPxY site in SUSD4 is essential for binding to NEDD4 ubiquitin ligases, the PPxY might have a regulatory role in controlling the ubiquitin ligase activity. A survey of the expression of HECT-ubiquitin ligases shows that different members of the NEDD4 subfamily are broadly expressed in the mouse brain, however with only partially overlapping patterns (**Figure S8**, http://mouse.brain-map.org, Allen Brain Atlas). *Nedd4* and *Wwp1* are the most broadly expressed and are found in neurons that also express *Susd4*, such as hippocampal neurons, inferior olivary neurons in the brainstem and cerebellar PCs. Thus, SUSD4 is a tether for ubiquitin ligases of the NEDD4 family and might modulate their activity in neurons.

SUSD4 regulates activity-dependent degradation of GLUA2

Ubiquitination is a post-translational modification essential for the regulation of protein turnover and trafficking in cells (Tai and Schuman, 2008). The NEDD4 family of ubiquitin ligases are known to ubiquitinate and target for degradation many key signaling molecules, including GLUA1- and GLUA2-containing AMPA receptors (Widagdo et al., 2017). SUSD4 binding to NEDD4 ubiquitin ligases, the lack of LTD at PF/PC synapses and our analysis of evoked quantal events thus suggested the involvement of SUSD4 in the regulation of postsynaptic receptor numbers, in particular, GLUA2-containing receptor numbers. Further evidence came from co-immunolabeling experiments using an anti-GLUA2 and an anti-VGLUT2 antibody on cerebellar sections followed by high-resolution microscopy. Several GLUA2 clusters of varying sizes were detected in close association with each VGLUT2 presynaptic bouton corresponding to CF synapses, while very small and dense GLUA2 clusters were found in the rest of the molecular layer corresponding mostly to GLUA2 clusters at the PF/PC synapses (**Figure 5A**). No obvious change in GLUA2 distribution in the molecular layer in *Susd4* KO mice was found when compared to WT controls, in accordance with normal basal transmission in PF/PC synapses. Quantitative analysis of the GLUA2 clusters associated with VGLUT2 labelled CF presynaptic boutons did not reveal a significant change in the total mean intensity of GLUA2 clusters per CF presynaptic bouton (**Figure 5A**). However, the proportion of CF presynaptic boutons with no GLUA2 cluster was smaller in juvenile *Susd4* KO mice than in WT mice (**Figure 5A**), partially explaining the increase in the amplitude of quantal EPSCs and CF transmission (**Figure 3E**).

Our model implied that a tripartite complex could be formed between SUSD4, NEDD4 ubiquitin ligases and GLUA2-containing AMPA receptors. To test this, we first co-expressed GLUA2 with various HA-tagged SUSD4 constructs (**Figure 5B**) in heterologous HEK293 cells and performed co-immunoprecipitation experiments (**Figure 5C**). GLUA2 and the ubiquitin ligase NEDD4 could both be found in extracts obtained after affinity-purification of the HA-tagged full length (FL-) SUSD4, while both were absent if HA-tagged FL-SUSD4 was replaced by a control transmembrane protein, PVRL3α (**Figure 5C**). NEDD4 interaction was absent when the SUSD4ΔC_T construct lacking the intracellular domain was used but not with the SUSD4ΔN_T construct lacking the extracellular domain, further confirming the binding of NEDD4 ubiquitin ligases to the intracellular domain of SUSD4. Strong co-immunoprecipitation of GLUA2 was detected in affinity-purified extracts from cells expressing the HA-tagged extracellular domain of SUSD4 alone (SUSD4N_T construct), showing that this domain is sufficient for GLUA2 interaction.

Conversely, binding to GLUA2 of a SUSD4 construct lacking the extracellular domain (SUSD4ΔN_T) was lower than the binding of the extracellular domain alone (SUSD4N_T), but was not completely abrogated, showing the cooperation of several domains of SUSD4 for the binding to GLUA2 (**Figure 5C**). In transfected cultured hippocampal neurons, clusters of GFP-tagged SUSD4 partially colocalize with GLUA2 clusters in spines (**Figure 5D**). Altogether our results suggest that SUSD4 acts as an adaptor protein that targets NEDD4 ubiquitin ligases to GLUA2-containing AMPA receptors to regulate their synaptic numbers.

If SUSD4 is involved in the targeting of AMPA receptors to RAB7-containing endolysosomal compartments for degradation, then it should also be found in RAB7-containing endolysosomal compartments. Co-transfection experiments in HeLA cells followed by immunolabeling showed that indeed SUSD4 is found in several intracellular compartments including the RAB7-positive endolysosomal compartments. Mutation of the PY binding site in SUSD4 decreases the colocalization of SUSD4 with RAB7 further suggesting a link between binding to NEDD4 ubiquitin ligases and SUSD4 localization in the degradation compartments (**Figure S9**). Given the role of NEDD4 ubiquitin ligases in the regulation of substrate degradation, SUSD4 could thus regulate GLUA2-containing AMPA receptor degradation. Indeed, total levels of GLUA2 are greatly reduced in HEK293 cells overexpressing SUSD4 when compared to control cells overexpressing a control transmembrane protein PVRL3α (**Figure 5** and **S10**). Lack of LTD in *Susd4* KO mice suggests that SUSD4 regulation of GLUA2 degradation is activity-dependent in neurons. To assess this, we set up a biochemical assay in which we induced chemical LTD (cLTD) in acute cerebellar slices (Kim et al., 2017) and measured total protein levels either in control conditions or with inhibitors of the proteasome and lysosomes (to estimate the GLUA2 degraded pool, **Figure 5E**). Total GLUA2 levels were not significantly different on average between WT and *Susd4* KO cerebellar slices in basal conditions, in accordance with our morphological and electrophysiological analysis of PF/PC synapses (**Figure S11**). In slices from WT mice, chemical induction of cLTD induced a significant reduction in total GLUA2 protein levels (**Figure 5E**). This reduction was prevented by incubation with the proteasome inhibitor MG132 and the lysosomal inhibitor leupeptin, showing that it corresponds to the pool of GLUA2 degraded in an activity-dependent manner (**Figure 5E**). In slices from *Susd4* KO mice, this activity-dependent degradation of GLUA2 was completely absent. Furthermore, the chemical induction of LTD did not change the total protein levels of another synaptic receptor highly present at PF/PC postsynaptic densities, GLURδ2 (GRID2), either in slices from WT or from *Susd4* mice (**Figure 5E** and **S11**). Thus, SUSD4 specifically controls the activity-dependent degradation of GLUA2 subunits during synaptic LTD.

Discussion

Our study shows that the CCP domain containing protein SUSD4 starts to be expressed in various neurons of the mammalian central nervous system when synapses are formed and mature. SUSD4 can bind both ubiquitin ligases of the NEDD4 family through its C-terminus domain and the GLUA2 AMPA receptor subunit, thus allowing the formation of a tripartite complex. *Susd4* loss-of-function in mice leads to deficient activity-dependent degradation of GLUA2 AMPA receptor subunits, lack of synaptic LTD in cerebellar PCs and impaired motor coordination and adaptation learning.

SUSD4 promotes long-term synaptic depression

The choice between recycling of AMPA receptors to the membrane or targeting to the endolysosomal compartment for degradation is key for the regulation of the number of AMPA receptors at synapses, as well as for the direction and degree of activity-dependent synaptic plasticity (Ehlers, 2000; Lee et al., 2002). Blocking trafficking of AMPA receptors through recycling endosomes, for example using a RAB11 mutant, prevents LTP in neurons (Park et al., 2004). Conversely, blocking the sorting of AMPA receptors to the endolysosomal compartment, for example using a RAB7 mutant, impairs LTD in hippocampal CA1 pyramidal neurons and cerebellar PCs (Fernandez-Monreal et al., 2012; Kim et al., 2017). Further support for the role of receptor degradation comes from mathematical modeling showing that in cerebellar PCs LTD depends on the regulation of the total pool of glutamate receptors (Kim et al., 2017). The GLUA2 AMPA receptor subunit, and its regulation, is of particular importance for LTD (Diering and Huganir, 2018). Phosphorylation in its C-terminal tail and the binding of molecular partners such as PICK1 and GRIP1/2 is known to regulate endocytosis and recycling (Bassani et al., 2012; Chiu et al., 2017; Fiuza et al., 2017), and mutations in some of the phosphorylation sites leads to impaired LTD (Chung et al., 2003). The molecular partners regulating the targeting for degradation of GLUA2 subunits in an activity-dependent manner during LTD remain to be identified. Our study shows that loss-of-function of *Susd4* leads both to loss of LTD and of activity-dependent degradation of GLUA2 subunits. Furthermore, loss-of-function of *Susd4* facilitates LTP of PF/PC synapses, and SUSD4 localization to RAB7 compartments is partly dependent on its binding to NEDD4 ubiquitin ligases. Overall our results support a model in which, during LTD, a specific molecular machinery containing SUSD4 promotes targeting of GLUA2-containing AMPA receptors to the degradation compartment in an activity-dependent manner, away from the recycling pathway that promotes LTP.

SUSD4 is a tether for NEDD4 E3 ubiquitin ligases

The degradation of specific targets such as neurotransmitter receptors must be regulated in a stimulus-dependent and synapse-specific manner in neurons, to ensure proper long-term synaptic plasticity, learning and memory (Tai and Schuman, 2008). How is this level of specificity achieved? Ubiquitination is a post-translational modification that has been shown to regulate protein degradation or signaling depending on the type of the ubiquitin chain added to lysines on the substrate protein. This modification is catalyzed by hundreds of different E3 ubiquitin ligases that belong to several families distinguished by their structure, mode of action and substrate selectivity (Zheng and Shabek, 2017). The family of HECT E3 ubiquitin ligases contains 28 enzymes including the NEDD4 subgroup that is characterized by an N-terminal C2 domain, several WW domains and the catalytic HECT domain. This subgroup of E3 ligases adds K63 ubiquitin chains to their substrate, a modification that promotes sorting to the endolysosomal compartment for degradation (Boase and Kumar, 2015). Our affinity-purification experiments identified SUSD4 as a binding partner for HECT ubiquitin ligases of the NEDD4 family and the mutation of the binding motifs in SUSD4 do not increase the amount of SUSD4 protein in cells suggesting that SUSD4 degradation itself is not regulated by NEDD4 ligases. Adaptor proteins that regulate both activation and substrate binding have been described for several E3 ligases. The activity of NEDD4 ligases depends on the opening of a closed conformation that can be controlled by the binding of several WW domains to PY motifs (Chen et al., 2017). Interestingly, mutation of only one of the two PY motifs of SUSD4 completely abrogates binding to NEDD4 while

mutation on the other one only partially impairs it. Thus, SUSD4 could act as an adaptor protein that regulates NEDD4 E3 ligases activity by changing their conformation.

Adaptor proteins can also regulate substrate binding and thus participate in the specificity of signaling through E3 ubiquitin ligases. NEDD4 E3 ligases are highly expressed in neurons in the mammalian brain and have many known substrates, including ion channels and the GLUA1 AMPA receptor subunit. Their activity and substrate selectivity thus need to be finely tuned. Both GLUA1 and GLUA2 AMPA receptor subunits are ubiquitinated on lysine residues in their intracellular tails in an activity-dependent manner (Lin et al., 2011; Lussier et al., 2011; Schwarz et al., 2010; Widagdo et al., 2015). Mutation of these lysine residues decreases localization of GLUA1 and GLUA2 AMPA receptor subunits in the endolysosomal compartment in neurons (Widagdo et al., 2015). On the contrary, GLUA1 and GLUA2 subunits lack any obvious intracellular direct binding motif to the WW domain of NEDD4 ubiquitin ligases and thus an adaptor molecule would be necessary for ubiquitination by these enzymes. SUSD4 could act as a chaperone for NEDD4 binding to the GLUA2 subunit, its ubiquitination and subsequent targeting to the endolysosomal compartment for degradation. While direct modulation of GLUA2 ubiquitination by SUSD4 remains to be demonstrated, the formation of this complex could provide a simple mechanism to regulate the specificity of action of NEDD4 ubiquitin ligases in neurons and proper control of LTD. Indeed, loss-of-function of *Susd4* leads to misregulation of GLUA2 activity-dependent degradation, but does not affect regulation of another postsynaptic receptor, GRID2. The SUSD4-dependent complex could be used to increase the efficiency of GLUA2 ubiquitination since it has been shown recently that membrane tethering and polymerization increases activity of NEDD4 ubiquitin ligases (Mund and Pelham, 2018). The presence of four CCP domains in the extracellular domain of SUSD4 also suggests that it could bind other proteins extracellularly. In particular, it was previously shown that SUSD4 can bind the C1Q globular domain of the complement protein C1 (Holmquist et al., 2013), a domain that is also found in presynaptic proteins of the C1Q family known for their role in synapse formation and function (Sigoillot et al., 2015; Südhof, 2018; Yuzaki, 2011). SUSD4 could thus enable fine spatiotemporal regulation of the activity of HECT ubiquitin ligases and the degradation of GLUA2-containing AMPA receptors in a trans-synaptic manner.

SUSD4 and neurodevelopmental disorders

The 1q41-42 deletion syndrome is characterized by many symptoms including intellectual deficiencies and seizures, and in a high majority of the cases the microdeletion encompasses the *Susd4* gene (Rosenfeld et al., 2011). A *Susd4* copy number variation has been identified in a patient with ASD (Cuscó et al., 2009). *Susd4* was recently identified amongst the 124 genes with genome wide significance for *de novo* mutations in a cohort of more than 10,000 patients with ASD or intellectual deficiencies (Coe et al., 2019). The *GRIA2* gene (coding for the GLUA2 subunit) has been found as an ASD susceptibility gene (Satterstrom et al., 2018) and mutations or misregulation of ubiquitin ligases have been found in many models of ASDs or intellectual deficiencies (Cheon et al., 2018; Lee et al., 2018; Satterstrom et al., 2018). For example, ubiquitination of GLUA1 by NEDD4-2 is impaired in neurons from a model of Fragile X syndrome (Lee et al., 2018). Understanding the precise molecular mechanisms underlying the activity-dependent degradation of GLUA2 by the SUSD4/NEDD4 complex will thus be of particular importance for our understanding of the etiology of these neurodevelopmental disorders.

Mutations in the *Susd4* gene could contribute to the etiology of neurodevelopmental disorders by impairing synaptic plasticity. Deficits in LTD such as the one found in the *Susd4* KO mice are a common feature of several mouse models of ASDs (Auerbach et al., 2011; Baudouin et al., 2012; Piochon et al., 2014). *Susd4* loss-of-function leads to motor impairments, a symptom that is also found in ASD patients (Fournier et al., 2010). Long-term synaptic plasticity has been proposed as a mechanism for learning and memory. While *in vivo* evidence for the role of LTP in these processes has accumulated, the role of LTD is still discussed (Andersen et al., 2017; Kakegawa et al., 2018; Raymond and Medina, 2018; Schonewille et al., 2011). Because of the broad expression of SUSD4 and of ubiquitin ligases of the NEDD4 subfamily in the mammalian central nervous system, this complex is likely to control LTD at many synapse types and its misregulation might lead to impairments in many learning and memory paradigms. Manipulation of SUSD4's function will thus now provide the means to test the relevance of LTD in many behavioral paradigms and its implication in the etiology of neurodevelopmental disorders.

Acknowledgments: The authors wish to thank all the personnel from the CIRB Imaging facility, in particular P. Mailly for help with the design of the macro for GLUA2 quantification and Estelle Anceaume for image acquisition (panel 1C). We also thank the personnel from the CIRB, INCI and chronobiotron CNRS UMS 3415, IBPS and IBENS animal facilities. We would like to thank Philippe Marin for advice on proteomics analysis. Mass spectrometry experiments were carried out using facilities of the Functional Proteomics Platform of Montpellier. **Funding:** This work was supported by funding from: ATIP-AVENIR program (RSE11005JSA to FS), Idex PSL ANR-10-IDEX-0001-02 PSL*(FS), ANR 9139SAMA90010901 (to FS and PI), ANR-15-CE37-0001-01 CeMod (to PI and FS), Fondation pour la Recherche Médicale Equipe FRM DEQ20150331748 (FS) and DEQ20140329514 (PI), and European Research Council ERC consolidator grant SynID 724601 (to FS). KI was supported by a PhD grant from the Ecole des Neurosciences de Paris (ENP) and the ENS Labex MemoLife (ANR-10-LABX-54 MEMO LIFE). JV and LR-R were supported by ANR-10-LABX-BioPsy (ANR-11-IDEX-0004-02) and ENP Foundation.

Contributions: FS, PI, LR-R, IG-C and KI designed the study and the experiments. IG-C, KI, MC, AK, FAG, JV, MS, ST, MA, OV, YN, AD, FS, SMS and MV performed the experiments, and collected the data; AT and J-LB provided the SUSD4 knockout mice and conceptual advice; FS and IG-C wrote the first draft of the manuscript; all authors read the manuscript and KI, MC, AK, MS, SMS, MV, AD, J-LB, PI and LR-R revised the manuscript.

Competing interests: Authors declare no competing interests.

Data and materials availability: All data is available in the main text or the supplementary materials.

Supplementary Information:
Materials and Methods
Figs. S1 to S11
Tables 1 and S1

References

Andersen, N., Krauth, N., and Nabavi, S. (2017). Hebbian plasticity in vivo: relevance and induction. Curr. Opin. Neurobiol. *45*, 188–192.

Anggono, V., and Huganir, R.L. (2012). Regulation of AMPA receptor trafficking and synaptic plasticity. Curr. Opin. Neurobiol. *22*, 461–469.

Atluri, P.P., and Regehr, W.G. (1996). Determinants of the Time Course of Facilitation at the Granule Cell to Purkinje Cell Synapse. J. Neurosci. *16*, 5661–5671.

Auerbach, B.D., Osterweil, E.K., and Bear, M.F. (2011). Mutations causing syndromic autism define an axis of synaptic pathophysiology. Nature *480*, 63–68.

Badura, A., Verpeut, J.L., Metzger, J.W., Pereira, T.D., Pisano, T.J., Deverett, B., Bakshinskaya, D.E., and Wang, S.S.-H. (2018). Normal cognitive and social development require posterior cerebellar activity. Elife *7*, 1–36.

Bassani, S., Cingolani, L.A., Valnegri, P., Folci, A., Zapata, J., Gianfelice, A., Sala, C., Goda, Y., and Passafaro, M. (2012). The X-Linked Intellectual Disability Protein TSPAN7 Regulates Excitatory Synapse Development and AMPAR Trafficking. Neuron *73*, 1143–1158.

Baudouin, S.J., Gaudias, J., Gerharz, S., Hatstatt, L., Zhou, K., Punnakkal, P., Tanaka, K.F., Spooren, W., Hen, R., De Zeeuw, C.I., et al. (2012). Shared synaptic pathophysiology in syndromic and nonsyndromic rodent models of autism. Science (80-.).

Binda, F., Dorgans, K., Reibel, S., Sakimura, K., Kano, M., Poulain, B., and Isope, P. (2016). Inhibition promotes long-Term potentiation at cerebellar excitatory synapses. Sci. Rep. *6*, 1–12.

Boase, N.A., and Kumar, S. (2015). NEDD4: The founding member of a family of ubiquitin-protein ligases. Gene *557*, 113–122.

Bolliger, M.F., Martinelli, D.C., and Sudhof, T.C. (2011). The cell-adhesion G protein-coupled receptor BAI3 is a high-affinity receptor for C1q-like proteins. Proc. Natl. Acad. Sci. *108*, 2534–2539.

Brechet, A., Buchert, R., Schwenk, J., Boudkkazi, S., Zolles, G., Siquier-Pernet, K., Schaber, I., Bildl, W., Saadi, A., Bole-Feysot, C., et al. (2017). AMPA-receptor specific biogenesis complexes control synaptic transmission and intellectual ability. Nat. Commun. *8*.

Buitrago, M.M., Schulz, J.B., Dichgans, J., and Luft, A.R. (2004). Short and long-term motor skill learning in an accelerated rotarod training paradigm. Neurobiol. Learn. Mem. *81*, 211–216.

Cajigas, J., Will, T., and Schuman, E.M. (2010). Protein homeostasis and synaptic plasticity. EMBO J. *29*, 2746–2752.

Chen, Z., Jiang, H., Xu, W., Li, X., Dempsey, D.R., Zhang, X., Devreotes, P., Wolberger, C., Amzel, L.M., Gabelli, S.B., et al. (2017). A Tunable Brake for HECT Ubiquitin Ligases. Mol. Cell *66*, 345-357.e6.

Cheon, S., Dean, M., and Chahrour, M. (2018). The ubiquitin proteasome pathway in neuropsychiatric disorders. Neurobiol. Learn. Mem. 106791.

Chiu, S.L., Diering, G.H., Ye, B., Takamiya, K., Chen, C.M., Jiang, Y., Niranjan, T., Schwartz,

C.E., Wang, T., and Huganir, R.L. (2017). GRASP1 Regulates Synaptic Plasticity and Learning through Endosomal Recycling of AMPA Receptors. Neuron *93*, 1405-1419.e8.

Choquet, D., and Triller, A. (2013). The dynamic synapse. Neuron *80*, 691–703.

Chung, H.J., Steinberg, J.P., Huganir, R.L., and Linden, D.J. (2003). Requirement of AMPA receptor GluR2 phosphorylation for cerebellar long-term depression. Science (80-.). *300*, 1751–1755.

Coe, B.P., Stessman, H.A.F., Sulovari, A., Geisheker, M.R., Bakken, T.E., Lake, A.M., Dougherty, J.D., Lein, E.S., Hormozdiari, F., Bernier, R.A., et al. (2019). Neurodevelopmental disease genes implicated by de novo mutation and copy number variation morbidity. Nat. Genet. *51*, 106–116.

Coesmans, M., Weber, J.T., De Zeeuw, C.I., and Hansel, C. (2004). Bidirectional parallel fiber plasticity in the cerebellum under climbing fiber control. Neuron *44*, 691–700.

Collingridge, G.L., Peineau, S., Howland, J.G., and Wang, Y.T. (2010). Long-term depression in the CNS. Nat. Rev. Neurosci. *11*, 459–473.

Crepel, F., Mariani, J., and Delhaye-Bouchaud, N. (1976). Evidence for a multiple innervation of purkinje cells by climbing fibers in the immature rat cerebellum. J. Neurobiol. *7*, 567–578.

Cuscó, I., Medrano, A., Gener, B., Vilardell, M., Gallastegui, F., Villa, O., González, E., Rodríguez-Santiago, B., Vilella, E., Del Campo, M., et al. (2009). Autism-specific copy number variants further implicate the phosphatidylinositol signaling pathway and the glutamatergic synapse in the etiology of the disorder. Hum. Mol. Genet. *18*, 1795–1804.

Davies, B., Brown, L.A., Cais, O., Watson, J., Clayton, A.J., Chang, V.T., Biggs, D., Preece, C., Hernandez-Pliego, P., Krohn, J., et al. (2017). A point mutation in the ion conduction pore of AMPA receptor GRIA3 causes dramatically perturbed sleep patterns as well as intellectual disability. Hum. Mol. Genet. *26*, 3869–3882.

Diering, G.H., and Huganir, R.L. (2018). The AMPA Receptor Code of Synaptic Plasticity. Neuron *100*, 314–329.

Ehlers, M.D. (2000). Reinsertion or degradation of AMPA receptors determined by activity-dependent endocytic sorting. Neuron *28*, 511–525.

Fernandez-Monreal, M., Brown, T.C., Royo, M., and Esteban, J.A. (2012). The Balance between Receptor Recycling and Trafficking toward Lysosomes Determines Synaptic Strength during Long-Term Depression. J. Neurosci. *32*, 13200–13205.

Fiuza, M., Rostosky, C., Parkinson, G., Bygrave, A., Halemani, N., Baptista, M., Milosevic, I., and Hanley, J.G. (2017). PICK1 regulates AMP receptor endocytosis via direct interaction with AP2 a-appendage and dynamin. Rockefeller Univ. Press J. Cell Biol *216*, 3323–3338.

Fournier, K.A., Hass, C.J., Naik, S.K., Lodha, N., and Cauraugh, J.H. (2010). Motor coordination in autism spectrum disorders: A synthesis and meta-analysis. J. Autism Dev. Disord. *40*, 1227–1240.

Gao, Z., Van Beugen, B.J., and De Zeeuw, C.I. (2012). Distributed synergistic plasticity and cerebellar learning. Nat. Rev. Neurosci. *13*, 619–635.

Gendrel, M., Rapti, G., Richmond, J.E., and Bessereau, J.-L. (2009). A secreted complement-

control-related protein ensures acetylcholine receptor clustering. Nature *461*, 992–996.

Gotow, T., and Sotelo, C. (1987). Postnatal development of the inferior olivary complex in the rat: IV. Synaptogenesis of GABAergic afferents, analyzed by glutamic acid decarboxylase immunocytochemistry. J.Comp Neurol. *263*, 526–552.

Gutierrez-Castellanos, N., Da Silva-Matos, C.M., Zhou, K., Canto, C.B., Renner, M.C., Koene, L.M.C., Ozyildirim, O., Sprengel, R., Kessels, H.W., and De Zeeuw, C.I. (2017). Motor Learning Requires Purkinje Cell Synaptic Potentiation through Activation of AMPA-Receptor Subunit GluA3. Neuron *93*, 409–424.

Hashimoto, K., and Kano, M. (2003). Functional differentiation of multiple climbing fiber inputs during synapse elimination in the developing cerebellum. Neuron *38*, 785–796.

Hirai, H., Pang, Z., Bao, D., Miyazaki, T., Li, L., Miura, E., Parris, J., Rong, Y., Watanabe, M., Yuzaki, M., et al. (2005). Cbln1 is essential for synaptic integrity and plasticity in the cerebellum. Nat. Neurosci. *8*, 1534–1541.

Hirano, T. (2018). Regulation and Interaction of Multiple Types of Synaptic Plasticity in a Purkinje Neuron and Their Contribution to Motor Learning. Cerebellum *17*, 756–765.

Holmquist, E., Okroj, M., Nodin, B., Jirström, K., and Blom, A.M. (2013). Sushi domain-containing protein 4 (SUSD4) inhibits complement by disrupting the formation of the classical C3 convertase. FASEB J. *27*, 2355–2366.

Holt, G.R., and Douglas, J. (1996). Comparison of Discharge Variability Visual Cortex Neurons. J. Neurophysiol. *75*, 1806–1814.

Ichise, T., Kano, M., Hashimoto, K., Yanagihara, D., Nakao, K., Shigemoto, R., Katsuki, M., and Aiba, a (2000). mGluR1 in cerebellar Purkinje cells essential for long-term depression, synapse elimination, and motor coordination. Science *288*, 1832–1835.

Ito, M. (2001). Cerebellar Long-Term Depression: Characterization, Signal Transduction, and Functional Roles. Physiol. Rev. *81*, 1143–1195.

Ito, M. (2006). Cerebellar circuitry as a neuronal machine. Prog. Neurobiol. *78*, 272–303.

Ito, M., and Kano, M. (1982). Long-lasting depression of parallel fiber-Purkinje cell transmission induced by conjunctive stimulation of parallel fibers and climbing fibers in the cerebellar cortex. Neurosci. Lett. *33*, 253–258.

Kakegawa, W., Mitakidis, N., Miura, E., Abe, M., Matsuda, K., Takeo, Y.H., Kohda, K., Motohashi, J., Takahashi, A., Nagao, S., et al. (2015). Anterograde C1ql1 signaling is required in order to determine and maintain a single-winner climbing fiber in the mouse cerebellum. Neuron *85*, 316–330.

Kakegawa, W., Katoh, A., Narumi, S., Miura, E., Motohashi, J., Takahashi, A., Kohda, K., Fukazawa, Y., Yuzaki, M., and Matsuda, S. (2018). Optogenetic Control of Synaptic AMPA Receptor Endocytosis Reveals Roles of LTD in Motor Learning. Neuron *99*, 985-998.e6.

Kashiwabuchi, N., Ikeda, K., Araki, K., Hirano, T., Shibuki, K., Takayama, C., Inoue, Y., Kutsuwada, T., Yagi, T., Kang, Y., et al. (1995). Impairment of Motor Coordination, Purkinje Cell Synapse Formation, and Cerebellar Long-Term Depression in GluRd2 Mutant Mice. Cell *81*, 245–252.

Kayakabe, M., Kakizaki, T., Kaneko, R., Sasaki, A., Nakazato, Y., Shibasaki, K., Ishizaki, Y., Saito, H., Suzuki, N., Furuya, N., et al. (2014). Motor dysfunction in cerebellar Purkinje cell-specific vesicular GABA transporter knockout mice. Front. Cell. Neurosci. *7*, 1–11.

Kessels, H.W., and Malinow, R. (2009). Synaptic AMPA Receptor Plasticity and Behavior. Neuron *61*, 340–350.

Kim, T., Yamamoto, Y., and Tanaka-Yamamoto, K. (2017). Timely regulated sorting from early to late endosomes is required to maintain cerebellar long-term depression. Nat. Commun. *8*.

Konnerth, A., Llanot, I., and Armstrongt, C.M. (1990). Synaptic currents in cerebellar Purkinje cells. Neurobiology *87*, 2662–2665.

Lalonde, R., and Strazielle, C. (2001). Motor performance and regional brain metabolism of spontaneous murine mutations with cerebellar atrophy. *125*, 103–108.

Lee, K.Y., Jewett, K.A., Chung, H.J., and Tsai, N.P. (2018). Loss of fragile X protein FMRP impairs homeostatic synaptic downscaling through tumor suppressor p53 and ubiquitin E3 ligase Nedd4-2. Hum. Mol. Genet. *27*, 2805–2816.

Lee, S.H., Liu, L., Wang, Y.T., and Sheng, M. (2002). Clathrin adaptor AP2 and NSF interact with overlapping sites of GluR2 and play distinct roles in AMPA receptor trafficking and hippocampal LTD. Neuron *36*, 661–674.

Lee, S.H., Simonetta, A., and Sheng, M. (2004). Subunit rules governing the sorting of internalized AMPA receptors in hippocampal neurons. Neuron *43*, 221–236.

Lefort, J.M., Vincent, J., Tallot, L., Jarlier, F., De Zeeuw, C.I., Rondi-Reig, L., and Rochefort, C. (2019). Impaired cerebellar Purkinje cell potentiation generates unstable spatial map orientation and inaccurate navigation. Nat. Commun. *10*, 1–13.

Leto, K., Arancillo, M., Becker, E.B.E., Buffo, A., Chiang, C., Ding, B., Dobyns, W.B., Dusart, I., Haldipur, P., Hatten, M.E., et al. (2016). Consensus Paper: Cerebellar Development. The Cerebellum *15*, 789–828.

Lin, A., Hou, Q., Jarzylo, L., Amato, S., Gilbert, J., Shang, F., and Man, H.Y. (2011). Nedd4-mediated AMPA receptor ubiquitination regulates receptor turnover and trafficking. J. Neurochem. *119*, 27–39.

Lussier, M.P., Nasu-Nishimura, Y., and Roche, K.W. (2011). Activity-dependent ubiquitination of the AMPA receptor subunit GluA2. J. Neurosci. *31*, 3077–3081.

Martin, S., Chamberlin, A., Shinde, D.N., Hempel, M., Strom, T.M., Schreiber, A., Johannsen, J., Ousager, L.B., Larsen, M.J., Hansen, L.K., et al. (2017). De Novo Variants in GRIA4 Lead to Intellectual Disability with or without Seizures and Gait Abnormalities. Am. J. Hum. Genet. *101*, 1013–1020.

Matsuda, K., Miura, E., Miyazaki, T., Kakegawa, W., Emi, K., Narumi, S., Fukazawa, Y., Ito-Ishida, A., Kondo, T., Shigemoto, R., et al. (2010). Cbln1 is a ligand for an orphan glutamate receptor delta2, a bidirectional synapse organizer. Science *328*, 363–368.

Matsuda, S., Kakegawa, W., Budisantoso, T., Nomura, T., Kohda, K., and Yuzaki, M. (2013). Stargazin regulates AMPA receptor trafficking through adaptor protein complexes during long-term depression. Nat. Commun. *4*, 1–15.

Mund, T., and Pelham, H.R. (2018). Substrate clustering potently regulates the activity of WW-HECT domain– containing ubiquitin ligases. J. Biol. Chem. *293*, 5200–5209.

Nakayama, M., Suzuki, E., Tsunoda, S. -i., and Hama, C. (2016). The Matrix Proteins Hasp and Hig Exhibit Segregated Distribution within Synaptic Clefts and Play Distinct Roles in Synaptogenesis. J. Neurosci. *36*, 590–606.

Nicoll, R.A. (2017). A Brief History of Long-Term Potentiation. Neuron *93*, 281–290.

Park, M., Penick, E., Edwards, J., Kauer, J., and Ehlers, M.D. (2004). Recycling Endosomes Supply AMPA Receptors for Long-term Potentiation. Science (80-.). *305*, 1972–1975.

Penn, A.C., Zhang, C.L., Georges, F., Royer, L., Breillat, C., Hosy, E., Petersen, J.D., Humeau, Y., and Choquet, D. (2017). Hippocampal LTP and contextual learning require surface diffusion of AMPA receptors. Nature *549*, 384–388.

Piochon, C., Kloth, A.D., Grasselli, G., Titley, H.K., Nakayama, H., Hashimoto, K., Wan, V., Simmons, D.H., Eissa, T., Nakatani, J., et al. (2014). Cerebellar plasticity and motor learning deficits in a copy-number variation mouse model of autism. Nat. Commun. *5*, 1–12.

Raymond, J.L., and Medina, J.F. (2018). Computational Principles of Supervised Learning in the Cerebellum. Annu. Rev. Neurosci. *41*, 233–253.

Rochefort, C., Arabo, A., Andre, M., Poucet, B., Save, E., and Rondi-Reig, L. (2011). Cerebellum Shapes Hippocampal Spatial Code. Science (80-.). *334*, 385–389.

Rondi-Reig, L., Delhaye-Bouchaud, N., Mariani, J., and Caston, J. (1997). Role of the inferior olivary complex in motor skills and motor learning in the adult rat. Neuroscience *77*, 955–963.

Rosenfeld, J.A., Lacassie, Y., El-Khechen, D., Escobar, L.F., Reggin, J., Heuer, C., Chen, E., Jenkins, L.S., Collins, A.T., Zinner, S., et al. (2011). New cases and refinement of the critical region in the 1q41q42 microdeletion syndrome. Eur. J. Med. Genet. *54*, 42–49.

Salpietro, V., Dixon, C.L., Guo, H., Bello, O.D., Vandrovcova, J., Efthymiou, S., Maroofian, R., Heimer, G., Burglen, L., Valence, S., et al. (2019). AMPA receptor GluA2 subunit defects are a cause of neurodevelopmental disorders. Nat. Commun. *10*.

Satterstrom, F.K., Kosmicki, J.A., Wang, J., and Breen, M.S. (2018). Large-scale exome sequencing study implicates both developmental and functional changes in the neurobiology of autism. 1–43.

Savas, J.N., De Wit, J., Comoletti, D., Zemla, R., Ghosh, A., and Yates, J.R. (2014). Ecto-Fc MS identifies ligand-receptor interactions through extracellular domain Fc fusion protein baits and shotgun proteomic analysis. Nat. Protoc. *9*, 2061–2074.

Schonewille, M., Gao, Z., Boele, H.J., Vinueza Veloz, M.F., Amerika, W.E., Šimek, A.A.M., De Jeu, M.T., Steinberg, J.P., Takamiya, K., Hoebeek, F.E., et al. (2011). Reevaluating the Role of LTD in Cerebellar Motor Learning. Neuron *70*, 43–50.

Schwarz, L.A., Hall, B.J., and Patrick, G.N. (2010). Activity-dependent ubiquitination of GluA1 mediates a distinct AMPA receptor endocytosis and sorting pathway. J. Neurosci. *30*, 16718–16729.

Sia, G.M., Clem, R.L., and Huganir, R.L. (2013). The human language-associated gene SRPX2 regulates synapse formation and vocalization in mice. Science (80-.). *342*, 987–991.

Sigoillot, S.M., Iyer, K., Binda, F., González-Calvo, I., Talleur, M., Vodjdani, G., Isope, P., and Selimi, F. (2015). The Secreted Protein C1QL1 and Its Receptor BAI3 Control the Synaptic Connectivity of Excitatory Inputs Converging on Cerebellar Purkinje Cells. Cell Rep. 820–832.

Sotelo, C. (2004). Cellular and genetic regulation of the development of the cerebellar system. Prog. Neurobiol. *72*, 295–339.

Stevens, B., Allen, N.J., Vazquez, L.E., Howell, G.R., Christopherson, K.S., Nouri, N., Micheva, K.D., Mehalow, A.K., Huberman, A.D., Stafford, B., et al. (2007). The Classical Complement Cascade Mediates CNS Synapse Elimination. Cell *131*, 1164–1178.

Stoodley, C.J. (2016). The Cerebellum and Neurodevelopmental Disorders. The Cerebellum *15*, 34–37.

Stoodley, C.J., D'Mello, A.M., Ellegood, J., Jakkamsetti, V., Liu, P., Nebel, M.B., Gibson, J.M., Kelly, E., Meng, F., Cano, C.A., et al. (2018). Author Correction: Altered cerebellar connectivity in autism and cerebellar-mediated rescue of autism-related behaviors in mice (Nature Neuroscience DOI: 10.1038/s41593-017-0004-1). Nat. Neurosci. *21*, 1016.

Südhof, T.C. (2018). Towards an Understanding of Synapse Formation. Neuron.

Suvrathan, A., Payne, H.L., and Raymond, J.L. (2016). Timing Rules for Synaptic Plasticity Matched to Behavioral Function. Neuron *92*, 959–967.

Tai, H., and Schuman, E.M. (2008). Ubiquitin , the proteasome and protein degradation in neuronal function and dysfunction. Nat. Rev. Neurosci. *9*.

Tsai, P.T., Hull, C., Chu, Y., Greene-Colozzi, E., Sadowski, A.R., Leech, J.M., Steinberg, J., Crawley, J.N., Regehr, W.G., and Sahin, M. (2012). Autistic-like behaviour and cerebellar dysfunction in Purkinje cell Tsc1 mutant mice. Nature *488*, 647–651.

Uemura, T., Lee, S.-J., Yasumura, M., Takeuchi, T., Yoshida, T., Ra, M., Taguchi, R., Sakimura, K., and Mishina, M. (2010). Trans-Synaptic Interaction of GluRδ2 and Neurexin through Cbln1 Mediates Synapse Formation in the Cerebellum. Cell *141*, 1068–1079.

Valera, A.M., Doussau, F., Poulain, B., Barbour, B., and Isope, P. (2012). Adaptation of Granule Cell to Purkinje Cell Synapses to High-Frequency Transmission. J. Neurosci. *32*, 3267–3280.

Volk, L., Chiu, S.-L., Sharma, K., and Huganir, R.L. (2015). Glutamate Synapses in Human Cognitive Disorders. Annu. Rev. Neurosci. *38*, 127–149.

Wang, S.S.H., Kloth, A.D., and Badura, A. (2014). The Cerebellum, Sensitive Periods, and Autism. Neuron *83*, 518–532.

Wang, Z., Liu, Z., Chen, X., Li, J., Yao, W., Huang, S., Gu, A., Lei, Q.-Y., Mao, Y., and Wen, W. (2019). A multi-lock inhibitory mechanism for fine-tuning enzyme activities of the HECT family E3 ligases. Nat. Commun. *10*.

Widagdo, J., Chai, Y.J., Ridder, M.C., Chau, Y.Q., Johnson, R.C., Sah, P., Huganir, R.L., and Anggono, V. (2015). Activity-Dependent ubiquitination of GluA1 and GluA2 regulates AMPA receptor intracellular sorting and degradation. Cell Rep. *10*, 783–795.

Widagdo, J., Guntupalli, S., Jang, S.E., and Anggono, V. (2017). Regulation of AMPA Receptor Trafficking by Protein Ubiquitination. Front. Mol. Neurosci. *10*, 1–10.

Xia, J., Chung, H.J., Wihler, C., Huganir, R.L., and Linden, D.J. (2000). Cerebellar long-term

depression requires PKC-regulated interactions between GluR2/3 and PDZ domain-containing proteins. Neuron *28*, 499–510.

Yuzaki, M. (2011). Cbln1 and its family proteins in synapse formation and maintenance. Curr. Opin. Neurobiol. *21*, 215–220.

Zheng, N., and Shabek, N. (2017). Ubiquitin Ligases: Structure, Function, and Regulation. Annu. Rev. Biochem. *86*, 129–157.

Zuo, J., De Jager, P.L., Takahashi, K.A., Jiang, W., Linden, D.J., and Heintz, N. (1997). Neurodegeneration in Lurcher mice caused by mutation in delta2 glutamate receptor gene [see comments]. Nature *388*, 769–773.

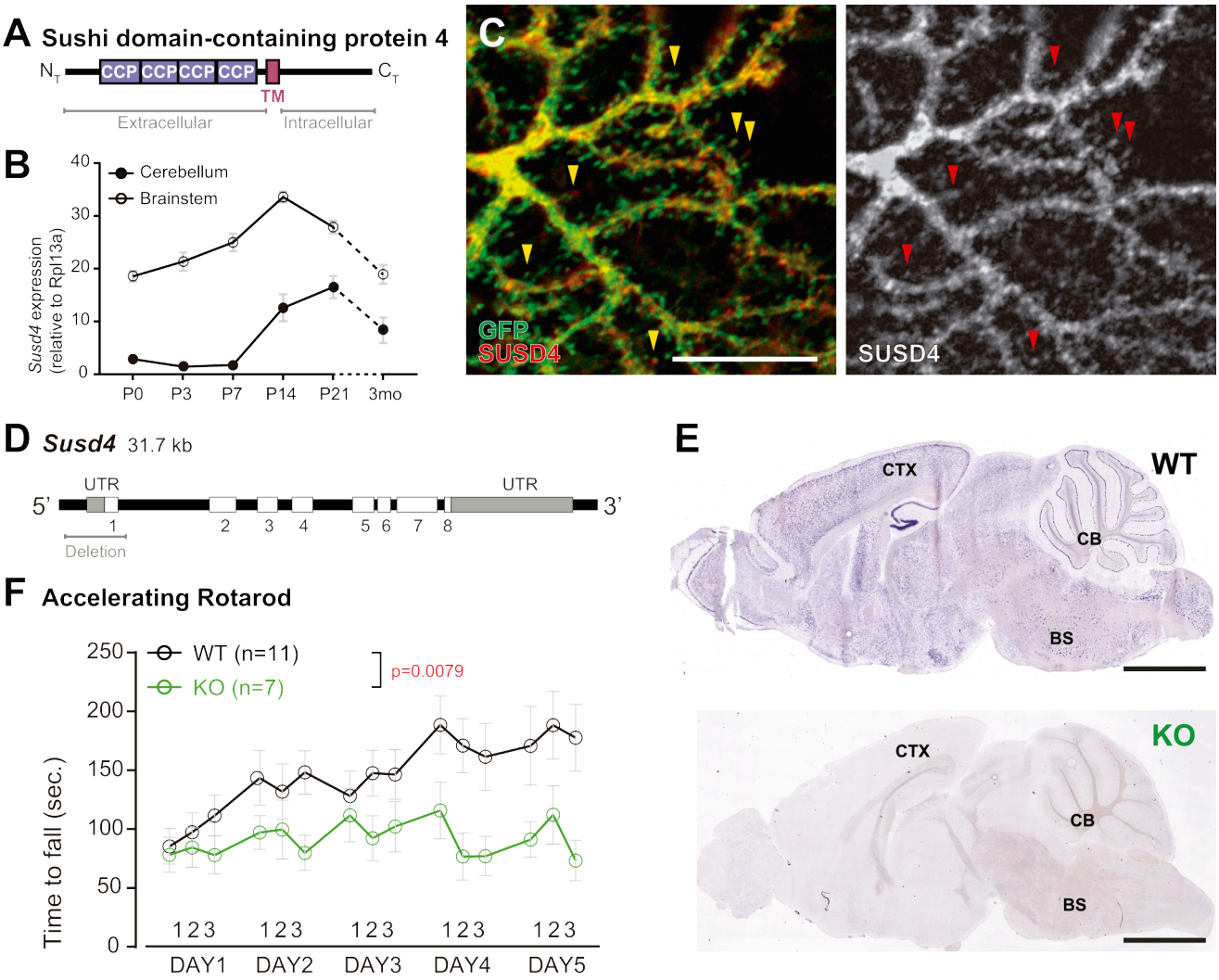
A
Sushi domain-containing protein 4
N_T
CCP CCP CCP CCP
C_T
TM
Extracellular
Intracellular
B
Cerebellum
Brainstem
Susd4 expression (relative to Rpl13a)
40
30
20
10
0
P0
P3
P7
P14
P21
3mo
C
GFP
SUSD4
SUSD4
D
Susd4 31.7 kb
5'
UTR
UTR
3'
1
2
3
4
5
6
7
8
Deletion
E
WT
CTX
CB
BS
KO
CTX
CB
BS
F
Accelerating Rotarod
WT (n=11)
KO (n=7)
p=0.0079
Time to fall (sec.)
250
200
150
100
50
0
1 2 3
1 2 3
1 2 3
1 2 3
1 2 3
DAY1
DAY2
DAY3
DAY4
DAY5

Figure 1. *Susd4* expression is necessary for motor coordination adaptation and learning.

(A) Diagram of the protein SUSD4 showing its domain organization with four extracellular Complement Control Protein (CCP) domains, one transmembrane (TM) domain and a cytoplasmic domain (C_T).

(B) Quantitative RT-PCR shows an increase in *Susd4* mRNA expression (relative to the housekeeping gene *Rpl13a*) during postnatal development in the cerebellum and in the brainstem. Mean ± s.e.m. (n=3 independent experiments). Extracts were prepared from tissue samples of mice aged 0 to 21 days (P0-21) and three months (3mo).

(C) HA-tagged SUSD4 is found in dendrites and distal dendritic spines in adult cerebellar Purkinje cells (arrowheads; anti-HA immunolabelling of parasagittal cerebellar sections obtained from adult mice after stereotaxic injection of AAV particles driving the expression of HA-SUSD4 and soluble GFP). Scale bar: 10 μm.

(D) Genomic structure of the *Susd4* gene. Labelled white boxes represent exons. Exon 1 is deleted in the *Susd4* loss-of-function mouse model.

(E) *In situ* hybridization experiments were performed on brain sections from one month-old wild-type (WT) and *Susd4* knockout (KO) mice to detect *Susd4* mRNA. *Susd4* expression was found in many regions of the brain in WT mice (see also **Figure S1**) including the cerebral cortex (CTX), the cerebellum (CB), and the brainstem (BS). No labeling was found in the brain of *Susd4* KO mice. Scale bars: 500 μm.

(F) Motor coordination and learning is deficient in adult *Susd4* knockout (KO) mice compared to age-matched WT littermates. Each mouse was tested three times per day during five consecutive days on an accelerating rotarod (4 to 40 r.p.m. in 10 minutes) and the time spent on the rotarod measured. Mean ± s.e.m. (WT n=11 and KO n=7, two-way ANOVA with repeated measures, Interaction (time and genotype): ** P=0.0079, F(14, 224) = 2.22; Time: **** P<0.0001, F(14, 224) = 3.469; Genotype: P=0.0553, F(1, 16) = 4.272).

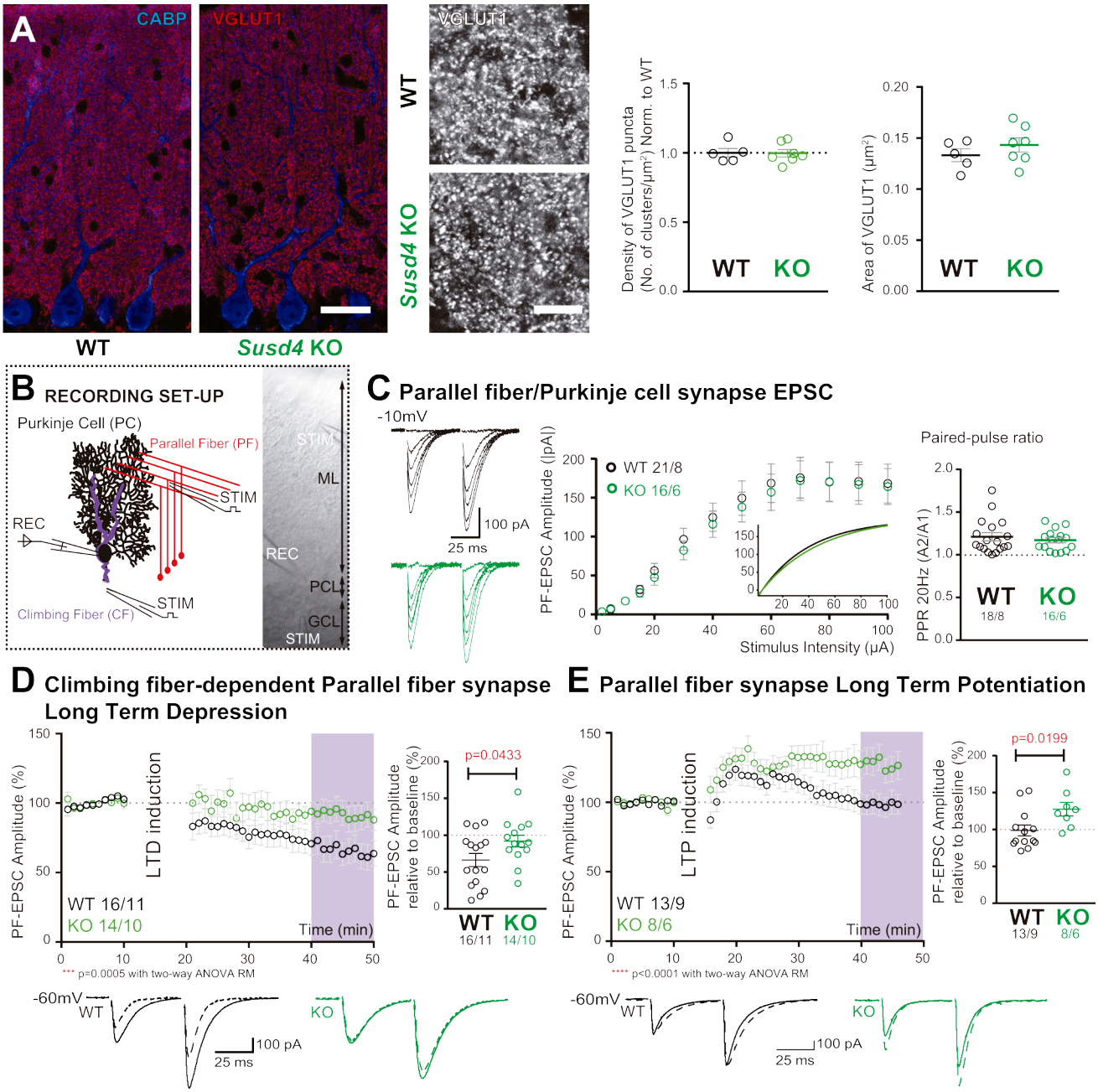
A
CABP
VGLUT1
WT
Susd4 KO
VGLUT1
WT
Susd4 KO
Density of VGLUT1 puncta (No. of clusters/μm²) Norm. to WT
Area of VGLUT1 (μm²)
WT KO
B RECORDING SET-UP
Purkinje Cell (PC)
Parallel Fiber (PF)
STIM
REC
Climbing Fiber (CF)
ML
PCL
GCL
C Parallel fiber/Purkinje cell synapse EPSC
-10mV
100 pA
25 ms
WT 21/8
KO 16/6
PF-EPSC Amplitude (|pA|)
Stimulus Intensity (μA)
Paired-pulse ratio
PPR 20Hz (A2/A1)
WT 18/8
KO 16/6
D Climbing fiber-dependent Parallel fiber synapse Long Term Depression
PF-EPSC Amplitude (%)
LTD induction
WT 16/11
KO 14/10
Time (min)
*** p=0.0005 with two-way ANOVA RM
PF-EPSC Amplitude relative to baseline (%)
p=0.0433
WT 16/11
KO 14/10
-60mV
WT
KO
100 pA
25 ms
E Parallel fiber synapse Long Term Potentiation
LTP induction
WT 13/9
KO 8/6
**** p<0.0001 with two-way ANOVA RM
p=0.0199
WT 13/9
KO 8/6

Figure 2. *Susd4* loss-of-function leads to deficient long-term depression and facilitated long-term potentiation of parallel fiber/Purkinje cell synapses.

(A) Quantitative analysis of the morphology of parallel fiber presynaptic boutons immunolabeled by an anti-VGLUT1 antibody (red) in Purkinje cells (anti-CABP, blue). Quantifications of the density and the area of the VGLUT1 clusters did not reveal any difference between *Susd4* KO and WT mice. Mean ± s.e.m. (WT n=5 and KO n=7; VGLUT1 clusters density: Mann-Whitney test, P>0.9999; area VGLUT1 clusters: Unpaired Student t-test, P=0.3089). Scale bars: 30 μm (left) and 10 μm (right).

(B) Diagram of the setup for patch-clamp recordings (REC) of Purkinje cells in 300 μm-thick parasagittal cerebellar slices. Parallel fiber and climbing fiber responses were elicited by electrical stimulation (STIM). ML: molecular layer; PCL: Purkinje cell layer; GCL: granule cell layer.

(C) Input-output curve of the parallel fiber/Purkinje cell transmission. The amplitude of the elicited EPSCs increases with the intensity of the stimulus and is not significantly different between *Susd4* KO and WT littermates. The fitted curves for each genotype are presented in the inset. Mean ± s.e.m. (WT n=21 cells, 8 mice and KO n=16 cells, 6 mice; Kolmogorov-Smirnov test, P=0.8793). Short-term plasticity of parallel fiber/Purkinje cell synapses is not affected by *Susd4* loss-of-function. Parallel fibers were stimulated twice at 50 ms interval and the paired-pulse ratio (PPR) was calculated by dividing the amplitude of the second peak divided by the amplitude of the first peak. Representative sample traces are presented. Mean ± s.e.m. (Mann-Whitney test, P=0.9052).

(D) Climbing fiber-dependent parallel fiber/Purkinje cell synapse long-term depression (LTD) is impaired in the absence of *Susd4* expression. LTD was induced by pairing stimulations of parallel fibers and climbing fibers at 100 milliseconds interval during 10 minutes at 0.5 Hz (**Figure S6C** and **D**). The amplitude of the PF EPSC was measured using two consecutive PF stimulation at 50 milliseconds interval. Representative sample traces are presented. Mean ± s.e.m. (WT n=16 cells, 11 mice and KO n=14 cells, 10 mice). Right: EPSC amplitudes from the last 10 minutes (purple) of recordings were used to calculate the LTD ratio relative to baseline (Two-tailed Wilcoxon Signed Rank Test with null hypothesis of 100: WT **p=0.0063; KO p=0.2676 Mann-Whitney test, WT vs KO *p=0.0433).

(E) Loss-of-function of *Susd4* facilitates parallel fiber/Purkinje cell synapse long-term potentiation (LTP). Tetanic stimulation of only parallel fibers at 0.3 Hz for 100 times (**Figure S6E** and **F**) induced LTP in *Susd4* KO Purkinje cells while inducing only a transient increase in parallel fiber transmission in WT Purkinje cells. Representative sample traces are presented. Mean ± s.e.m. (WT n=13 cells, 9 mice and KO n=8 cells, 6 mice. Right: EPSC amplitudes from the last 7 minutes (purple) were used to calculate the LTP ratio relative to baseline (Two-tailed Wilcoxon Signed Rank Test with null hypothesis of 100: WT p=0.5879; KO *p=0.0234; Mann-Whitney test, WT vs KO: *p=0.0199).

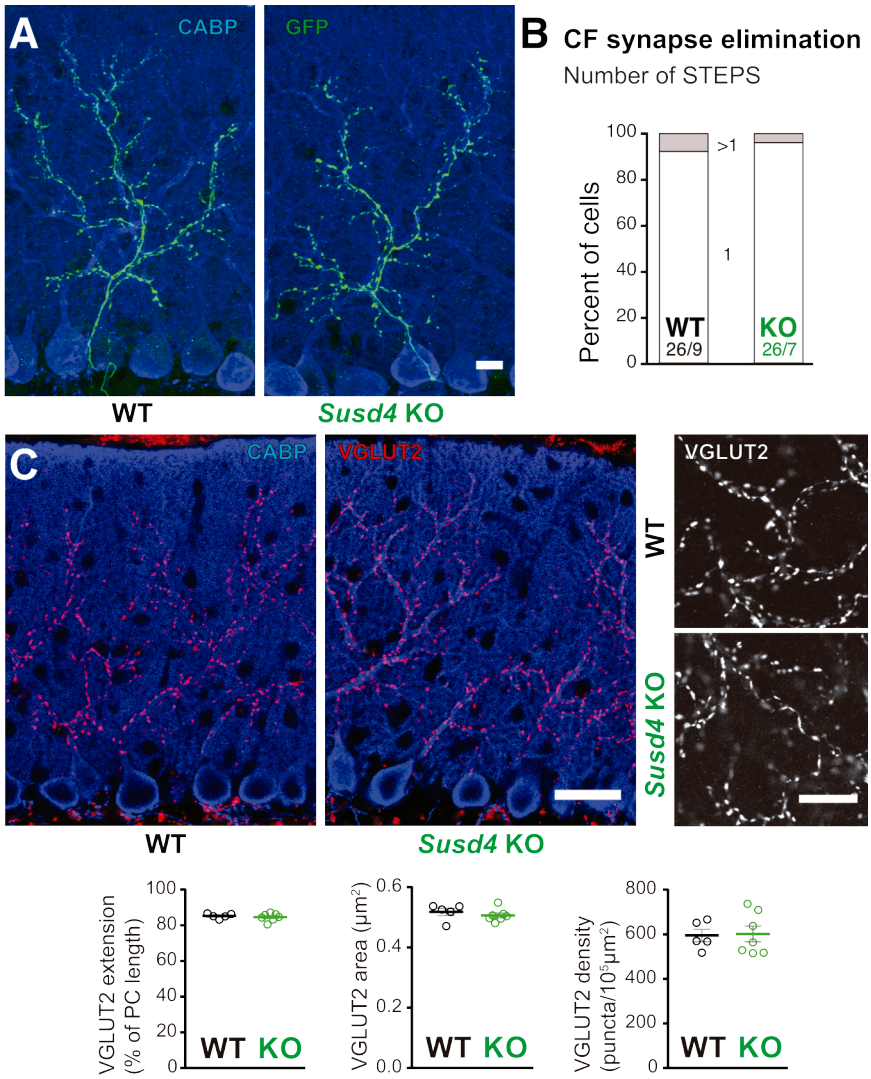

D Climbing fiber/Purkinje cell synapse EPSC

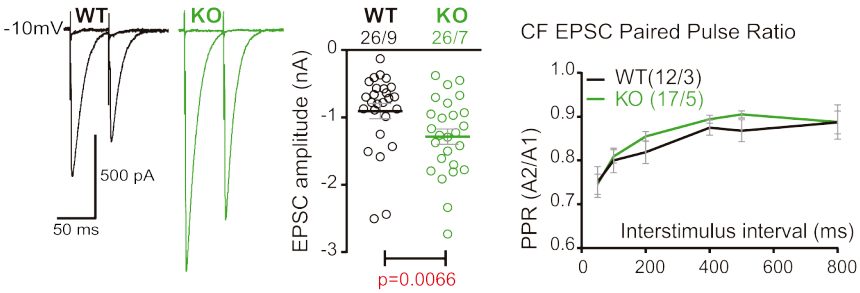

E Climbing Fiber Synapse: Delayed EPSC quanta

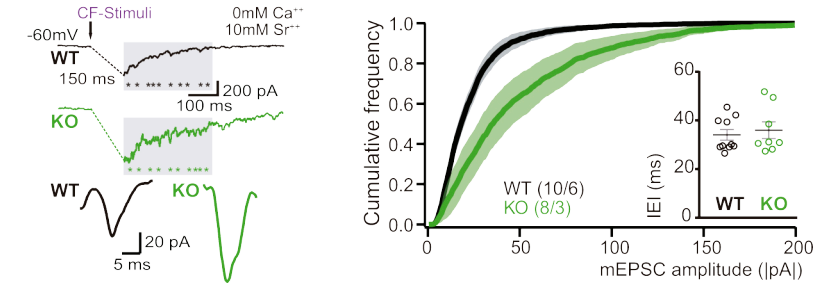

Figure 3. Transmission at the Climbing fiber/Purkinje cell synapses is increased in *Susd4* knockout mice.

(A) Left: Climbing fibers were visualized in *Susd4* WT and KO mice crossed with Htr5b-eGFP reporter mice (www.gensat.org) expressing the green fluorescent protein specifically in inferior olivary neurons. Anti-GFP and anti-CABP immunofluorescence was performed on parasagittal sections of P30 mice, and showed no qualitative differences in the absence of *Susd4* expression. Scale bar: 10 μm.

(B) Patch-clamp recordings of Purkinje cells showed a similar percentage of mono- (1 climbing fiber) and multi-innervation (>1 climbing fibers) of Purkinje cells in P30 *Susd4* KO and WT mice, as measured by the number of steps elicited by electrical stimulation of the climbing fibers. WT n=26 cells from 9 mice and KO n=26 cells from 7 mice (Chi-square test, P=0.5520).

(C) Climbing fiber presynaptic boutons were immunostained with an anti-VGLUT2 antibody in cerebellar sections from P30 WT and *Susd4* KO mice. The extension of the climbing fiber territory was calculated by measuring the extent of the VGLUT2 labeling relative to the height of the Purkinje cell dendritic tree (immunostained using an anti-CABP antibody, blue). Quantification of the mean density of VGLUT2 puncta and their mean area showed no differences between *Susd4* KO mice and their control littermates. Mean ± s.e.m. (WT n=5 and KO n=7; VGLUT2 extension: Mann-Whitney test, P=0.6389; VGLUT2 area: Unpaired Student t-test, p=0.4311; VGLUT2 density: Unpaired Student t-test, p=0.8925). Scale bars: 30 μm (left) and 10 μm (right).

(D) The amplitude of the climbing fiber elicited EPSC was increased in *Susd4* KO mice compared to WT littermates. (WT n=26 cells, 9 mice and KO n=26 cells, 7 mice, Mann-Whitney test, ** P=0.0066). Short-term synaptic plasticity of climbing fiber/Purkinje cell synapses was elicited by two consecutive stimulations at various intervals. No difference in the paired pulse ratios (PPR) was detected at any interval between *Susd4* KO mice and WT mice. Representative sample traces are presented. Mean ± s.e.m. (WT n=12 cells, 3 mice and KO n=17 cells, 5 mice; Kolmogorov-Smirnov test, P=0.1666; see also **Figure S7**).

(E) Delayed CF-EPSC quanta were evoked by CF stimulation in the presence of strontium instead of calcium to induce desynchronization of fusion events. Representative sample traces are presented. The cumulative probability for the amplitude of the events together with the individual amplitude values for each event show an increased amplitude associated with *Susd4* loss-of-function. Mean ± s.e.m. (WT n=10 cells, 6 mice and KO n=8 cells, 3 mice; Kolmogorov-Smirnov distribution test, *** P<0.0001). The individual frequency values for each cell (measured as interevent interval, IEI) present no differences between the genotypes. Mean ± s.e.m. (Mann Whitney test, P=0.6334; see also **Figure S7**).

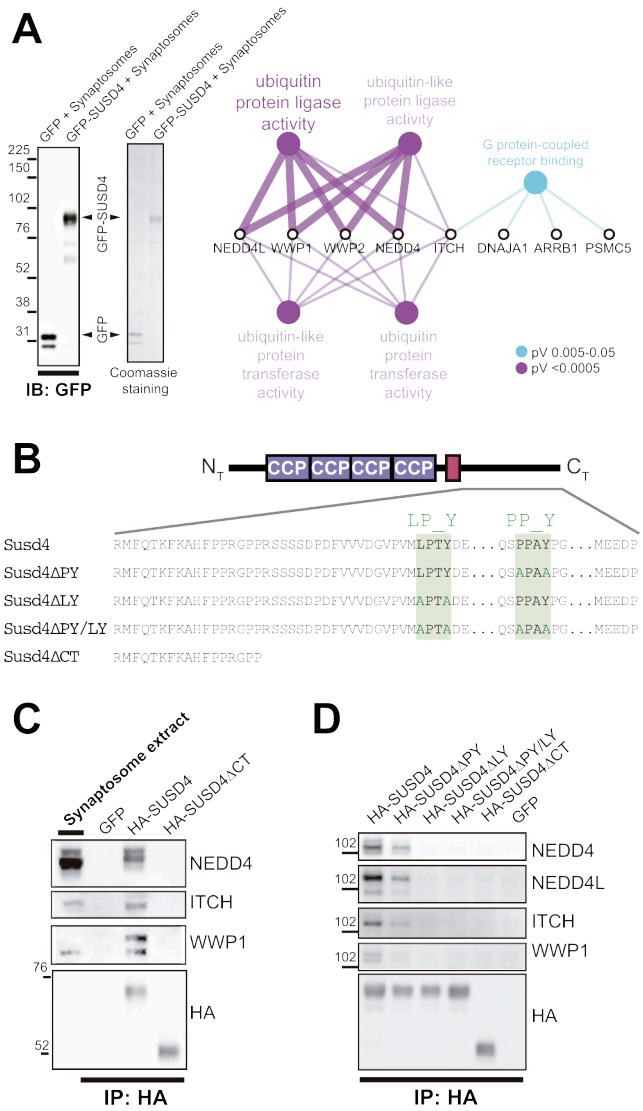
A
GFP + Synaptosomes
GFP-SUSD4 + Synaptosomes
225
150
102
76
52
38
31
GFP-SUSD4
GFP
IB: GFP
Coomassie staining
ubiquitin protein ligase activity
ubiquitin-like protein ligase activity
G protein-coupled receptor binding
NEDD4L
WWP1
WWP2
NEDD4
ITCH
DNAJA1
ARRB1
PSMC5
ubiquitin-like protein transferase activity
ubiquitin protein transferase activity
pV 0.005-0.05
pV <0.0005
B
N_T
CCP
CCP
CCP
CCP
C_T
LP_Y
PP_Y
Susd4 RMFQTKFKAHFPPRGPPRSSSSDPDFVVVDGVPVMLPTYDE...QSPPAYPG...MEEDP
Susd4ΔPY RMFQTKFKAHFPPRGPPRSSSSDPDFVVVDGVPVMLPTYDE...QSAPAAPG...MEEDP
Susd4ΔLY RMFQTKFKAHFPPRGPPRSSSSDPDFVVVDGVPVMAPTADE...QSPPAYPG...MEEDP
Susd4ΔPY/LY RMFQTKFKAHFPPRGPPRSSSSDPDFVVVDGVPVMAPTADE...QSAPAAPG...MEEDP
Susd4ΔCT RMFQTKFKAHFPPRGPP
C
Synaptosome extract
GFP
HA-SUSD4
HA-SUSD4ΔCT
NEDD4
ITCH
WWP1
76
52
HA
IP: HA
D
HA-SUSD4
HA-SUSD4ΔPY
HA-SUSD4ΔLY
HA-SUSD4ΔPY/LY
HA-SUSD4ΔCT
GFP
102
NEDD4
NEDD4L
ITCH
WWP1
HA
IP: HA

Figure 4. SUSD4 interacts with HECT E3 ubiquitin ligases.

(A) Mass spectrometry identification of SUSD4 interactors. Left: Affinity-purification from cerebellar synaptosomes was performed using either GFP-SUSD4 as a bait or GFP as a control. Proteins were then resolved using SDS-PAGE followed by immunoblot for anti-GFP and coomassie staining of proteins. Right: Gene Ontology (GO) enrichment analysis network (Molecular Function category) of the 28 candidate proteins (Cytoscape plugin ClueGO) identified after affinity-purification of cerebellar synaptosomes using GFP-SUSD4 as a bait followed by LC MS/MS. The Ubiquitin ligase activity term is significantly enriched due in particular to the identification of several members of the NEDD4 family of HECT-ubiquitin ligase. See also **Table 1**.

(B) Schematic representation of SUSD4 and different mutant constructs: SUSD4ΔPY (point mutation of the PPxY site); SUSD4ΔLY (point mutation of the LPxY); SUSD4ΔPY/LY (double mutant at both PPxY and LPxY) and SUSD4ΔC_T (lacking the cytoplasmic tail).

(C) Affinity-purification experiments followed by western blot analysis confirm the interaction of full length SUSD4 (HA-tagged, HA-SUSD4) with members of the NEDD4 family. This interaction is lost when the C-terminal tail of SUSD4 is deleted (HA-SUSD4ΔC_T) or when GFP is used instead of SUSD4 as a control.

(D) HEK293 cells were transfected with HA-SUSD4 full length, HA-SUSD4ΔPY, HA-SUSD4ΔLY, HA-SUSD4ΔPY/LY or HA-SUSD4ΔC_T or control GFP. Immunoprecipitation was then performed with an anti-HA antibody and extracts were probed for co-immunoprecipitation of the HECT ubiquitin ligases NEDD4, NEDD4L, ITCH and WWP1.

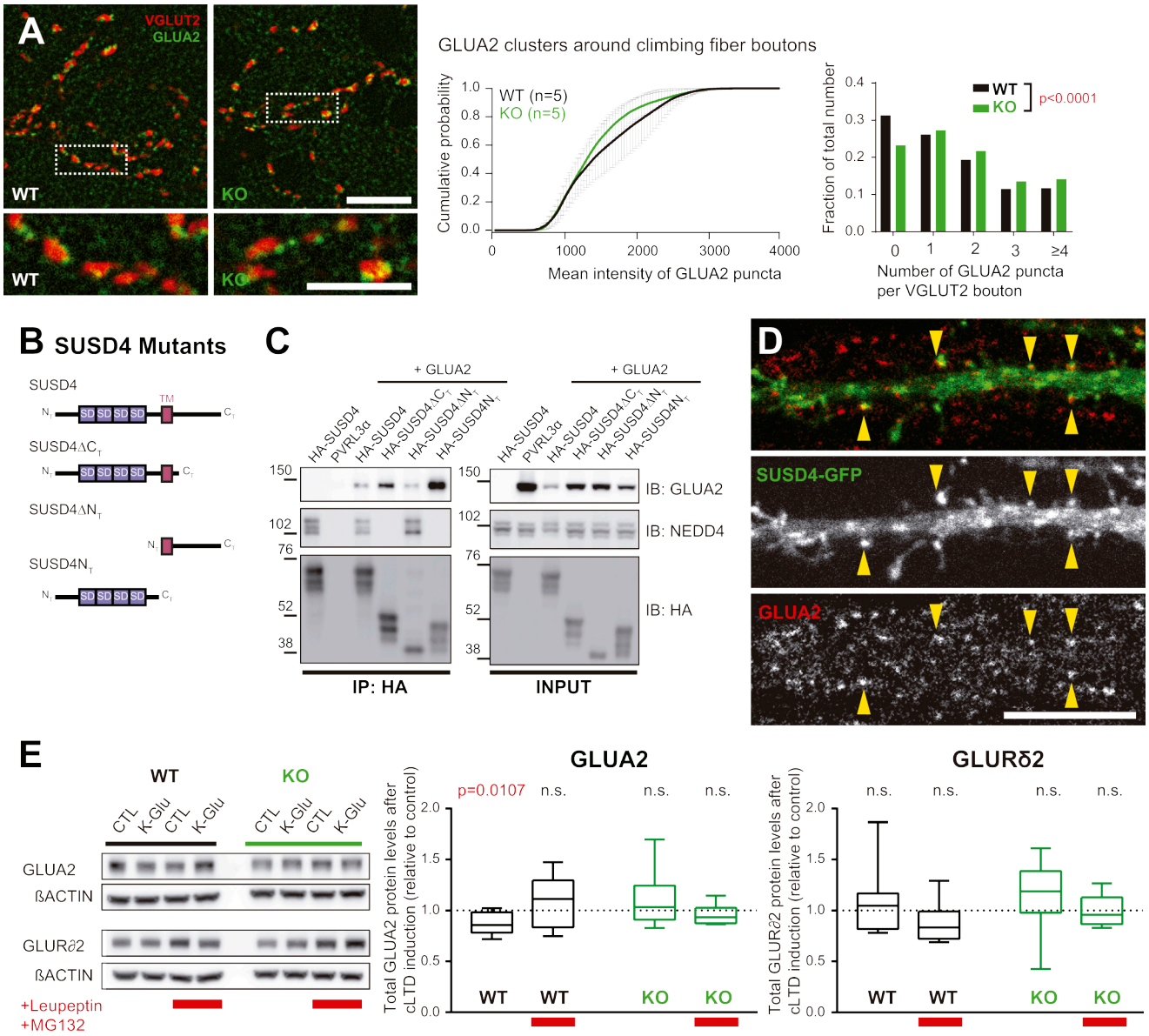
A
VGLUT2
GLUA2
WT
KO
WT
KO
GLUA2 clusters around climbing fiber boutons
Cumulative probability
WT (n=5)
KO (n=5)
Mean intensity of GLUA2 puncta
Fraction of total number
WT
KO
p<0.0001
Number of GLUA2 puncta per VGLUT2 bouton
B SUSD4 Mutants
SUSD4
SUSD4ΔC
SUSD4ΔN
SUSD4N
TM
C
+ GLUA2
HA-SUSD4
PVRL3α
HA-SUSD4ΔC
HA-SUSD4ΔN
HA-SUSD4N
IB: GLUA2
IB: NEDD4
IB: HA
IP: HA
INPUT
D
SUSD4-GFP
GLUA2
E
WT
KO
CTL
K-Glu
GLUA2
ßACTIN
GLURδ2
ßACTIN
+Leupeptin
+MG132
GLUA2
p=0.0107
n.s.
Total GLUA2 protein levels after cLTD induction (relative to control)
GLURδ2
Total GLURδ2 protein levels after cLTD induction (relative to control)

Figure 5. SUSD4 controls activity-dependent degradation of the AMPA receptor subunit GLUA2.

(A) The number of GLUA2 clusters (anti-GLUA2 immunolabeling, green) per climbing fiber presynaptic bouton (anti-VGLUT2 immunolabeling, red) and their intensity was quantified in cerebellar sections of juvenile *Susd4* KO mice and WT littermates. Scale bars: 30 μm (top); 15 μm (bottom). Cumulative plot for the mean GLUA2 intensity per VGLUT2 bouton shows no significant change between WT and KO. Mean ± s.e.m. (WT n= 5 and KO n= 5 mice. Kolmogorov-Smirnov test, P=0.5009). The distribution of the VGLUT2 boutons according to the number of associated GLUA2 clusters is significantly different between WT and KO (Chi-square contingency test, **** P<0.0001).

(B) Schematic representation of SUSD4 and different mutant constructs: SUSD4ΔC_T (lacking the cytoplasmic tail), SUSD4ΔN_T (lacking the extracellular domains) and SUSD4N_T (lacking the transmembrane and intracellular domains).

(C) SUSD4 interaction with GLUA2 and NEDD4. HEK293 cell extracts were transfected with HA-SUSD4 full length or HA-SUSD4ΔC_T or SUSD4ΔN_T or SUSD4N_T or control PVRL3α together with GLUA2. Immunoprecipitation was then performed with an anti-HA antibody and probed for co-immunoprecipitation of GLUA2 and the ubiquitin ligase NEDD4 (n=3 independent experiments).

(D) Mouse hippocampal neurons were transfected at 13 days *in vitro* (DIV13) with a GFP-tagged SUSD4 construct and immunostained at DIV17 for green fluorescent protein (GFP, green) to localize SUSD4 and for the endogenous GLUA2 subunit (anti-GLUA2, red). The yellow arrowheads indicate the spines containing SUSD4 and GLUA2. Scale bar: 10 μm.

(E) Activity-dependent degradation of GLUA2 was induced in cerebellar acute slices from *Susd4* WT mice using a protocol for chemical LTD (cLTD; K-Glu: K^+ 50mM and glutamate 10µM for 5 minutes followed by 30 minutes recovery). This degradation was absent when slices were incubated with 100μg/mL leupeptin and with 50μM MG132 (to inhibit lysosomal and proteasome degradation, respectively), or when slices were obtained from *Susd4* KO mice. Band intensities of GLUA2 and GLURδ2 were normalized to β-ACTIN. The ratios between levels with cLTD induction (K-Glu) and without cLTD induction (CTL) are represented. Mean ± s.e.m. Two-tailed Student's one sample t-test was performed on the ratios with a null hypothesis of 1, * P=0.0107, n.s.= not significant (n=8 independent experiments; see also **Figure S11**).